April 15, 1992

Spatial variation of a short-lived intermediate chemical species in a Couette reactor

R. Dennis Vigil, *University of Texas at Austin*
Q. Ouyang, *University of Texas at Austin*
Harry L. Swinney, *University of Texas at Austin*

Spatial variation of a shortlived intermediate chemical species in a Couette reactor

R. Dennis Vigil, Q. Ouyang, and Harry L. Swinney

Citation: The Journal of Chemical Physics **96**, 6126 (1992); doi: 10.1063/1.462655
View online: http://dx.doi.org/10.1063/1.462655
View Table of Contents: http://scitation.aip.org/content/aip/journal/jcp/96/8?ver=pdfcov
Published by the AIP Publishing

Spatial variation of a short-lived intermediate chemical species in a Couette reactor

R. Dennis Vigil, Q. Ouyang, and Harry L. Swinney
Center for Nonlinear Dynamics, Department of Physics, The University of Texas, Austin, Texas 78712

(Received 7 November 1991; accepted 7 January 1992)

We have conducted experiments and simulations of the spatial variation of a short-lived intermediate species (triiodide) in the autocatalytic oxidation of arsenite by iodate in a reactor that is essentially one dimensional—the Couette reactor. (This reactor consists of two concentric cylinders with the inner one rotating and the outer one at rest; reagents are continuously fed and removed at each end in such a way that there is no net axial flux and there are opposing arsenite and iodate gradients.) The predictions of a one-dimensional reaction–diffusion model, which has *no* adjustable parameters, are in good qualitative (and, in some cases, quantitative) agreement with experiments. Thus, the Couette reactor, which is used to deliberately create spatial inhomogeneities, can be exploited to enhance the recovery of short-lived intermediate species relative to that which can be obtained with either a batch or continuous-flow stirred-tank reactor.

I. INTRODUCTION

Continuous-flow stirred tank reactors (CSTR's) are widely used for both industrial and research applications. Much of their utility stems from their ability to sustain a homogeneous reaction far from thermodynamic equilibrium. If, however, the desired product is a short-lived intermediate species, then often the reactor must be maintained at a very narrow set of conditions that correspond to an unstable steady state in which the species is present in relatively high concentrations. The sensitivity of such systems to even the smallest perturbations in process variables (such as feed concentrations, flow rates, and temperature) requires that sophisticated process control strategies and hardware be used.[1–12]

Recently, an alternative approach to recovering short-lived intermediate species has been introduced by Ouyang *et al.*[13] This method employs a Couette cell as a chemical reactor. A Couette cell consists of a fluid confined to the annular region between two concentric cylinders, with one or both cylinders rotating (in the work of Ouyang *et al.* the outer cylinder was fixed). Above a critical Reynolds number R_c, the flow self-organizes into pairs of oppositely rotating toroidal vortices (Taylor vortices) stacked along the cylinder axis. At higher Reynolds numbers rapid radial and azimuthal mixing occurs within each Taylor vortex. Axial transport between neighboring vortices, however, occurs on a much longer time scale. If the reacting species (say A and B) are continuously fed at opposite ends of the cell (into the Taylor vortices nearest to the ends) and solution is removed at both ends at flow rates equal to the reactant feed rates so that there is no net mass transport in the axial direction, then a steady state will be reached in which the concentration of each species varies from one vortex to the next. Since there is to a good approximation no radial or azimuthal dependence on concentration, the axial transport can be described by a one-dimensional form of Fick's law, at least on length scales large compared to the size of a vortex.[14] The effective diffusivity, typically several orders of magnitude larger than molecular diffusion, depends upon the cylinder speed and is identical for all species due to the mechanical nature of the transport mechanism. A Couette cell, then, can be employed as a one-dimensional reaction–diffusion system (Couette reactor). The chemical reactants that are fed at opposite ends of the reactor diffuse toward each other, forming a reaction front at some point along its length. Within this steady reaction front, the short-lived species is present in a relatively high concentration, and it can be recovered by simply tapping it at the appropriate location along the length of the reactor and by replacing it with an equal volume of solvent so that there is no net axial flow. This recovery technique is in sharp contrast to those that employ stirred tanks. In a Couette reactor spatial inhomogeneities are deliberately created, preserved, and exploited rather than destroyed.

In the earlier work[13] the utility of a Couette reactor for recovering a short-lived species (HOCl) was demonstrated for the minimal chlorite–iodide reaction. The effects of several control parameters such as the cylinder rotation rate, the feed concentrations, and the removal rate of the intermediate species were studied. However, the concentration distribution along the length of the reactor could not be quantitatively determined for any particular species. In the present work we discuss the results of a Couette reactor experiment on another reaction: the acidic oxidation of arsenite by iodate. This simple system was chosen since the mechanism and reaction kinetics are fairly well understood. We have measured the concentration distribution of a particular intermediate species (triiodide) and have compared these results with the predictions of a reaction–diffusion model of a Couette reactor.

II. EXPERIMENTAL METHOD

A. The chemical reaction

In order to simplify our study, a homogeneous liquid-phase reaction with well-understood kinetics was chosen.

 0021-9606/92/086126-06$06.00

The acidic oxidation of arsenite by iodate can be modeled by the two-step mechanism,[15,16]

$$5I^- + IO_3^- + 6H^+ \rightarrow 3I_2 + 3H_2O, \quad (A)$$

$$H_3AsO_3 + I_2 + H_2O \rightarrow H_3AsO_4 + 2I^- + 2H^+. \quad (B)$$

If arsenite is in excess, the iodine produced in reaction (A) is quickly consumed by reaction (B), which is significantly faster than reaction (A), and the overall reaction is given by (A) + 3(B):

$$IO_3^- + 3H_3AsO_3 \rightarrow I^- + 3H_3AsO_4. \quad (C)$$

Note that iodide is a product in the net reaction and that it is also a reactant in the rate-limiting reaction (A). Therefore, the net reaction accelerates as iodide is produced (it is autocatalytic in I^-) and iodine is a short-lived species. The reaction rates of (A) and (B) have been previously studied and are given by[17]

$$r_A = [H^+]^2[IO_3^-][I^-](k_{A1} + k_{A2}[I^-]) \quad (1)$$

and[18]

$$r_B = k_B \frac{[I_2][H_3AsO_3]}{[I^-][H^+]}, \quad (2)$$

where the rate constants are given by[17] $k_{A1} = 8\times10^3\ M^{-3}\ s^{-1}$, $k_{A2} = 6\times10^8\ M^{-4}\ s^{-1}$, and[19] $k_B = 3.2\times10^{-2}\ Ms^{-1}$.

B. Apparatus

The Couette reactor (Fig. 1) consisted of a concentric inner rod (o.d. = 2.22 cm) and outer cylinder (i.d. = 2.54 cm, length = 20 cm). The outer cylinder was fixed by end plates, while the inner cylinder was able to rotate through bearings in the end plates and was connected to a precision motor by a rubber belt. Both pieces were made from optical glass. The reactor was arranged vertically along its main axis to facilitate the escape of bubbles. The arsenite solution was fed into the bottom vortex via a small hole in the bottom end plate by a precision piston pump (Pharmacia P-500). Solution was removed by an identical pump from the bottom of the reactor (opposite to the feed location) at a volumetric flow rate equal to the arsenite feed rate. Similarly, iodate solution was introduced into the uppermost vortex by the use of a precision pump. Therefore, the flow rate of the exit stream at the top of the reactor was self-adjusting (such that there was no net mass flux through the reactor) since the flow rates of the other three streams were fixed by precision pumps. The entire assembly was surrounded by a circulating water bath at 20 °C.

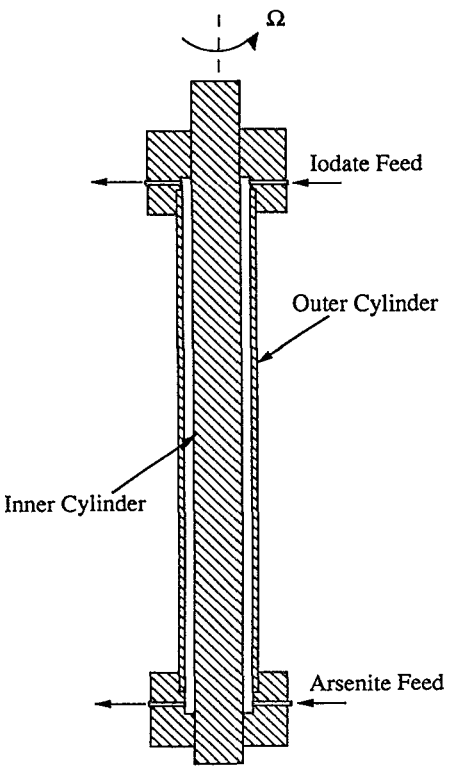

FIG. 1. Schematic of the Couette reactor showing configuration of feed and removal streams.

C. Data collection

The presence of iodine in the reactor was detected by using Thiodène (a soluble starch from Prolabo) as an indicator. Iodine, iodide, and Thiodène react to form a complex that absorbs light with wavelengths in the range 570–590 nm. However, neither the mechanism nor the rate law for this reaction is well-understood. It is widely believed that amylose is the component in starch that reacts with iodine and iodide to form the light-absorbing complex. Several investigators have studied the reaction between iodine, iodide, and amylose,[20–24] and their findings suggest the following approximate scenario. First, iodine and iodide react to form triiodide:

$$I_2 + I^- \rightleftarrows I_3^-, \quad (D)$$

with an equilibrium constant given by $K_{eq} = 770\ M^{-1}$. A complex is then formed by the reaction,

$$I_3^- + Am^- \rightleftarrows Am\cdot I_3^-, \quad (E)$$

where Am is amylose. Once the triodide–amylose complex is formed, it may react repeatedly to bind iodine molecules along the length of the amylose chain.

In view of the above considerations and in order to facilitate the comparison between simulation and experiment, we calibrated our optical absorption measurements in the following manner. First, several solutions with known initial concentrations of iodine and iodide were prepared with the fixed concentration ratio $[I^-]/[I_2] = 10$. The equilibrium concentration of the resulting triiodide was then calculated and a fixed amount of Thiodène (2 g/l) was added to the solution. The solution was placed in the reactor and the light absorption was measured. In this way we were able to construct a calibration curve (Fig. 2) relating the concentration of triodide (without starch) with the observed light absorption due to the triiodide–iodine–Thiodène complex.

Once the above calibration curve was constructed, it was possible to obtain an estimate of the triiodide concentration for a given set of experimental conditions. A high pressure sodium lamp with a peak intensity between 550–600 nm

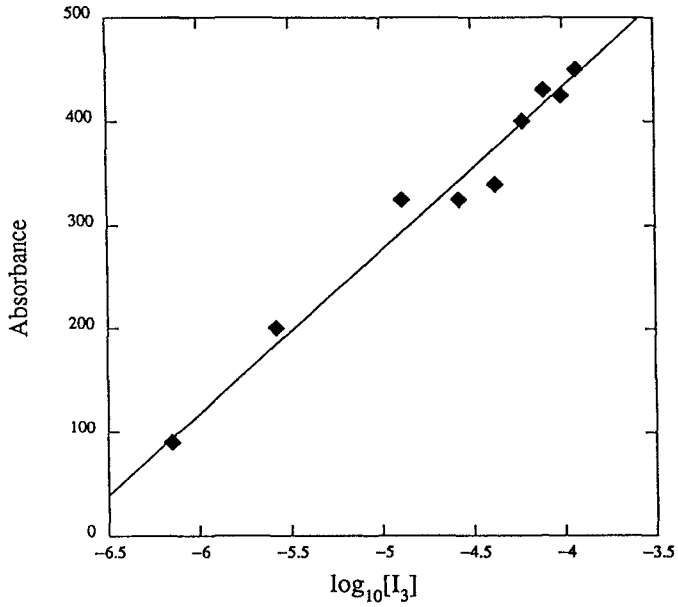

FIG. 2. Calibration curve for absorption measurements. The observed light absorbance between 550–600 nm is plotted as a function of the calculated equilibrium concentration of triiodide (in the absence of starch).

was used for illumination. The light from the lamp was passed through a lens in order to produce parallel light. A one-dimensional CCD array (with 4096 photodetectors) was used to acquire data for the light intensity as a function of axial position in the reactor, and the data were stored on an IBM PC-AT for later analysis.

III. NUMERICAL SIMULATIONS

Since fluid in each Taylor vortex can be considered to be well-mixed, we can approximate the reactor as a network of CSTR's connected in series (with flow in both directions), where each CSTR corresponds to a vortex. The flow rate of each species between adjacent CSTR's is proportional to the effective diffusion coefficient as well as the difference in concentration between the CSTR's. Since the rate laws are known for the component reactions (A) and (B), the concentration of species i in CSTR (vortex) j obeys the reaction–diffusion equation:

$$\frac{d[i]_j}{dt} = -r_{ij} + D_s\{([i]_{j+1} - [i]_j) + ([i]_{j-1} - [i]_j)\}, \quad (3)$$

where r_{ij} is the rate of reaction of species i (in vortex j). The term D_s is the scaled effective diffusivity, $D_s = D_{\text{eff}}(n/L)^2$, where n is the number of vortices and L is the reactor length. Three Reynolds number ratios were used in our study: $R/R_c = 2.5$, 5, and 10. The corresponding values of D_{eff} are given by[25] 0.0146, 0.0282, and 0.0783 cm^2/s.

The vortices at the ends of the reactor obey slightly different equations due to the feed and removal of reactants. These are given by

$$\frac{d[i]_1}{dt} = -r_{i1} + D_s([i]_2 - [i]_1) + k_{01}([i]_{\text{feed}} - [i]_1), \quad (4)$$

and

$$\frac{d[i]_{j\max}}{dt} = -r_{ij\max} + D([i]_{j\max-1} - [i]_{j\max}) + k_{02}([i]_{\text{feed}} - [i]_{j\max}), \quad (5)$$

where k_{01} and k_{02} are the scaled (by the volume of a single vortex) flow rates of the feed and removal streams at either end of the reactor. Since the iodine–iodide–triiodide reaction rapidly reaches equilibrium, it is not necessary to write a differential equation for triiodide. Within each vortex there are four species with unknown concentrations: iodate, iodide, iodine, and arsenite. Thus, a closed system of $4n$ ordinary differential equations with $4n$ unknowns can be constructed. For the Reynolds numbers used in this study the number of vortices is typically 75 but can vary depending on the Reynolds number history.[14,26] We note that the above reaction–diffusion model (with different boundary conditions) has been employed by Showalter to describe chemical waves in the arsenite–iodate system in a stagnant medium.[27]

This system of differential equations is stiff owing to the large difference in the rates of reaction of (A) and (B). It was therefore integrated using Gear's backward differentiation method. The integrations were performed with the following initial conditions: $[I_2]_j = [IO_3^-]_j = [AsO_3]_j = 0.0$ mol/l, $[I^-]_j = 1.0\times10^{-4}$ mol/l, and were carried out until steady-state conditions were met (a change of less than 0.1% in all variables).

IV. RESULTS AND DISCUSSION

The concentration profiles of arsenite, iodate, and triiodide obtained from a numerical simulation at one set of conditions corresponding to a typical experiment are shown in Figs. 3(a)–3(c). As we expect, the concentrations of arsenite and iodate decrease almost linearly as a function of the distance from their feed locations due to the imposed gradients. Furthermore, at a single intermediate location the concentrations of both arsenite and iodate are nearly zero, and this location is that at which a single peak occurs in the concentration of triiodide. These concentration profiles suggest that a chemical front occurs at this position and that intermediate species such as triiodide are present in relatively high concentrations. We emphasize that this state can be sustained indefinitely as long as reactants are continuously fed and removed at the boundaries. We have found that the width of the triiodide peak, which represents the chemical reaction front, was typically 10%–20% of the length of the reactor. The peak triodide concentration was 1–2 orders of magnitude smaller than the feed concentration of the limiting reagent, IO_3^-.

For comparison, we have performed numerical simulations of the temporal evolution of triiodide in a batch reactor [Fig. 3(d)]. This is a closed system and thus it cannot be sustained at a nonequilibrium steady state. Notice that the triiodide concentration undergoes an induction period,

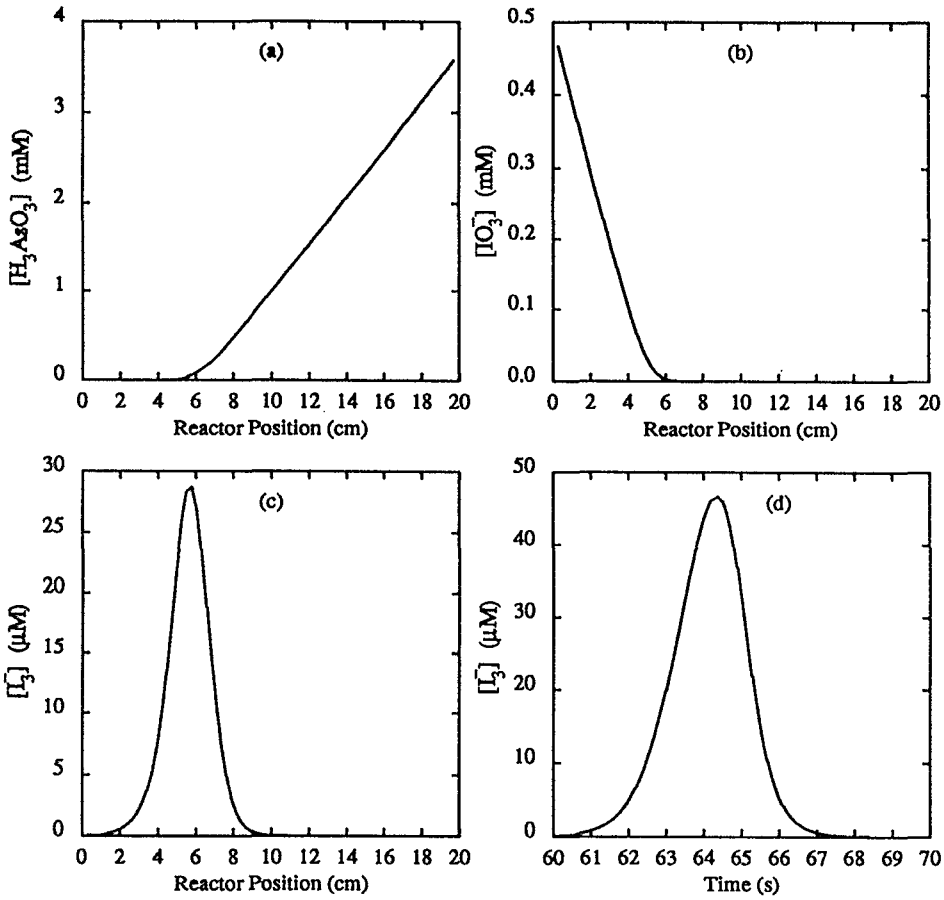

FIG. 3. Numerical simulation predictions of the (a) arsenite, (b) iodate, and (c) triiodide concentration distributions in the Couette reactor with $[H_3AsO_3]_f = 5.0$ mM, $[NaIO_3]_f = 1.0$ mM, $[I^-]_0 = 1.0\times10^{-4}$ mM, $[I_2]_0 = 0.0$, and $[H^+]_0 = 0.1$ M. Iodate was fed at position 0.0 cm and arsenite was fed at position 20.0 cm. The scaled feed stream flow rates were $K_{01} = K_{02} = 0.035\,s^{-1}$. (d) Results of a numerical simulation showing the time evolution of the triiodide concentration in a *batch* reactor during the acidic oxidation of arsenite by iodate. The following initial concentrations were used: $[NaIO_3]_0 = 0.001$ M, $[I^-]_0 = 1.0\times10^{-7}$ M, $[I_2]_0 = 0.0$ M, $[H_3AsO_3]_0 = 0.01$ M, and $[H^+]_0 = 0.1$ M.

reaches a maximum, and decays rapidly. It is only present in large concentrations for a few seconds. The maximum concentration and the shape of the pulse is similar to that observed in the Couette reactor under similar reactant concentrations. This comparison is suggestive of the utility of a Couette reactor. In a stirred batch reactor spatial fluctuations are destroyed and the concentrations of all reactants are time-dependent. In a Couette reactor, spatial inhomogeneities are created and, in a sense, the time dependence of the concentration of a species in a batch reactor is converted to a *spatial* distirbution that is *time-independent.*

This description of a Couette reactor is corroborated by experiment. For example, Fig. 4 shows a direct comparison of the simulation prediction with the experimental observation at a particular set of conditions. The numerical simulation gives excellent qualitative agreement and surprisingly good quantitative agreement with the data, especially considering that the model contains no adjustable parameters and that it is approximate due to the incomplete understanding of the nature of Thiodène and its interaction with iodine and iodide.

The location of the front depends strongly on the ratio of the feed stream concentrations, $[H_3AsO_3]_f/[NaIO_3]_f$. Fig-

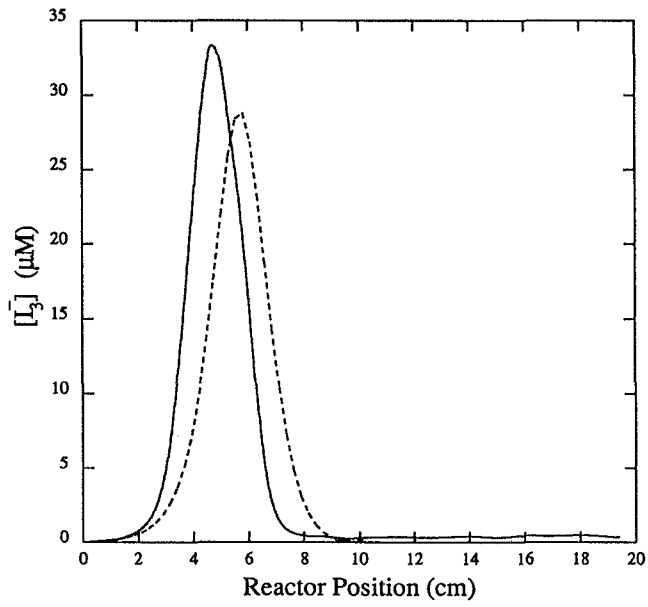

FIG. 4. A direct comparison of the predicted and observed triiodide concentration distribution under the same conditions as Fig. 3(c).

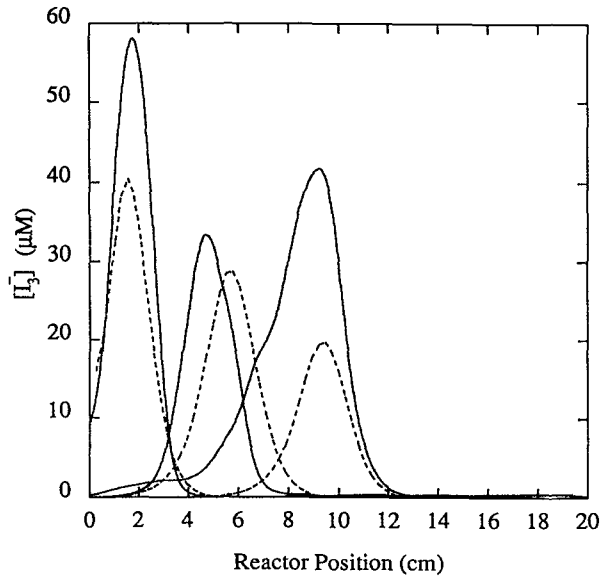

FIG. 5. Measured (solid lines) and predicted (dashed) triiodide concentration distributions along the length of the reactor for three feed concentration ratios, $[H_3AsO_3]_f/[NaIO_3]_f = 10$, 5, and 3 from left to right. In all three cases $R/R_c = 5$, $[H^+] = 0.1$ M, and $[NaIO_3] = 0.001$ M. Iodate was fed at reactor position 0.0 cm while arsenite was fed at 20.0 cm. Both were fed at 40 ml/h. The measurements were made after the system reached steady-state conditions (~ 1 h).

ure 5 shows a comparison of experiments and simulations at three sets of conditions. As the relative feed concentration of arsenite is increased, the front moves further away from the end of the reactor at which arsenite is fed, but the peak triiodide concentration and the width of the front do not vary greatly.

Figures 6(a)–6(d) show the effects of varying the Reynolds number and relative feed rate ratios on the triiodide concentrations. In both cases, the position and width of the reaction front do not vary greatly in the range that these parameters were studied. Indeed, it appears that the maxima of the triiodide concentrations are slightly more dependent on this variable. The weak dependence of the triiodide distribution on the Reynolds number is somewhat surprising. The effective diffusivity changes by a factor of 7 as R/R_c is increased from 2.5 to 10.0. One would expect that as D_{eff} is increased, that a broadening of the reaction front would occur due to the larger rate of axial transport. Nevertheless, such a broadening effect was *not* observed, in contrast to the findings with the minimal chlorite–iodide reaction.[17]

In conclusion, we have shown that a simple one-dimensional reaction–diffusion model can provide a semiquantitative description of the spatial structure in a Couette reactor. Our calculations and experiments show that short-lived species can be sustained indefinitely at relatively high concen-

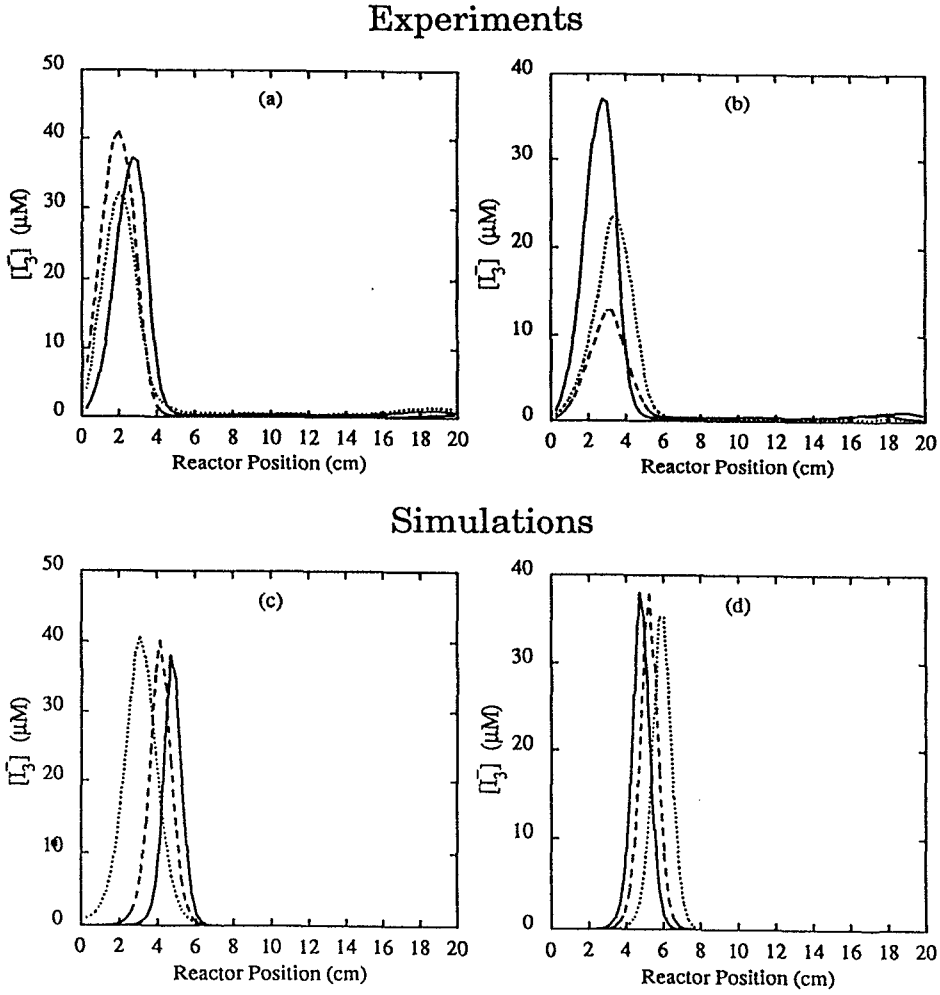

FIG. 6. The effects of varying the Reynolds number and the feed flow rates on the triiodide distribution in a Couette reactor. (a) Measured triiodide concentration distributions (three separate experiments) along the length of the reactor for $R/R_c = 2.5$ (solid), 5 (dashed) 10 (dots). In all cases $[H_3AsO_3]_f/[NaIO_3]_f = 10$, $[H^+] = 0.1$ M, and $[NaIO_3] = 0.001$ M. (c) Numerical simulations corresponding to the experiments in (a). (b) Measured triiodide concentration distributions along the length of the reactor for the three cases $k_{01}/k_{02} = 1.0$ (solid), 1.5 (dashed), and 1.67 (dots), where k_{01} and k_{02} are the flowrates of iodate and arsenite, respectively. In all three experiments $R/R_c = 2.5$, $[H^+] = 0.1$ M, and $[NaIO_3] = 0.001$ M. (d) Numerical simulations corresponding to the experiments in (b).

trations. Hence, the Couette reactor has promising applications in both basic and applied science. For example, the ability to recover short-lived intermediate species in significant concentrations may aid in the study of the mechanism and kinetics of important reactions. Furthermore, these intermediate species may have intrinsic value for the development of commercial products. Other potential applications might include the fractionation of polymers or copolymers for composition and molecular weight.

ACKNOWLEDGMENTS

We would like to acknowledge fruitful discussions with W. D. McCormick and Z. Noszticzius. This work is supported by the Department of Energy Office of Basic Energy Sciences. R. Dennis Vigil acknowledges the support provided by a Ford Foundation post-doctoral fellowship, administered by the National Research Council.

[1]R. Aris and N. R. Amundsen, Chem. Eng. Sci. **7**, 121 (1958).
[2]J. M. Douglas, *Process Dynamics and Control* (Prentice-Hall, Englewood Cliffs, NJ, 1972).
[3]J. S. Ding, S. Sharma, and D. Luss, Ind. Eng. Chem. Fundam. **13**, 76 (1974).
[4]M. Chang and R. A. Schmitz, Chem. Eng. Sci. **30**, 837 (1975).
[5]D. D. Bruns and J. E. Bailey, Chem. Eng. Sci. **30**, 755 (1975).
[6]S. M. Meerkov, IEEE Trans. Auto. Control **AC-25**, 755 (1980); **AC-27**, 485 (1982).
[7]R. Bellman, J. Bentsman, and S. M. Meerkov, J. Math. Anal. Appl. **91**, 152 (1983); **97**, 572 (1983).
[8]A. Cinar, J. Deng. S. M. Meerkov, and X. Shu, AIChE Annual Meeting, San Francisco, Paper No. 101b (1984).
[9]E. C. Zimmermann, M. Schell, and J. Ross, J. Chem. Phys. **81**, 1327 (1984).
[10]J. Kramer and J. Ross, J. Chem. Phys. **83**, 6234 (1985).
[11]M. Schell and J. Ross, J. Chem. Phys. **85**, 6489 (1986).
[12]J. P. Laplante, J. Phys. Chem. **93**, 3882 (1989).
[13]Q. Ouyang, H. L. Swinney, J. C. Roux, P. De Kepper, and J. Boissonade, AIChE. J. (in press).
[14]W. Y. Tam and H. L. Swinney, Phys. Rev. A **36**, 1374 (1987).
[15]J. Eggert and B. Scharnow, Z. Elektrochem. **27**, 455 (1921).
[16]P. DeKepper, I. R. Epstein, and K. Kustin, J. Am. Chem. Soc. **103**, 6121 (1981).
[17]H. A. Liebhafsky and G. M. Roe, Int. J. Chem. Kinet. **11**, 693 (1979).
[18]J. R. Roebuck, J. Phys. Chem. **6**, 365 (1902); **9**, 727 (1905).
[19]J. N. Pendlebury and R. H. Smith, Int. J. Chem. Kinet. **6**, 663 (1974).
[20]K. Hiromi, T. Shibaoka, and S. Ono, J. Bioichem. **68**, 205 (1970).
[21]J. C. Thompson and E. Hamori, J. Phys. Chem. **75**, 272 (1971).
[22]E. Hamori and M. C. Kallay, Biopolymers **11**, 475 (1972).
[23]A. Yamagishi, T. Imamura, and M. Fujimoto, Bull. Chem. Soc. Jpn. **45**, 2304 (1972).
[24]A. Cesáro, J. C. Benegas, and D. R. Ripoll, J. Phys. Chem. **90**, 2787 (1986).
[25]Q. Ouyang, PhD. thesis, L'Universite de Bordeaux, 40 (1989).
[26]D. Coles, J. Fluid Mech. **21**, 385 (1965).
[27]K. Showalter, in *Chemical Waves* in *Kinetics of Nonhomogeneous Processes*, edited by G. R. Freeman (Wiley, New York, 1987), pp. 776–780.